

Effects of Jet Decay Rate on Jet-Induced Loads on a Flat Plate

J.M. Kuhlman* and R.W. Warcup†
Old Dominion University, Norfolk, Va.

Experimental modeling of the interaction between a jet and an aircraft wing or fuselage in VTOL aircraft was undertaken using a cold jet exiting perpendicular to a flat plate in a uniform crossflow. Effects of jet decay rate and jet-to-crossflow velocity ratio, R , on the induced load distribution were investigated. Jet decay rate was increased by using cylindrical centerbodies submerged in the jet nozzle, which caused nonuniform initial jet velocity profiles. A quicker jet decay rate, corresponding to the presence of a centerbody, resulted in as much as a 45% reduction in the induced pressure loads on the plate. This has implications in interpretation of results from earlier VTOL model studies of jet-induced loads, where the jets have often had relatively slow decay rates due to uniform initial velocity profiles.

Nomenclature

c_p	= $(p - p_{no\ jet})/q_\infty$ = jet-induced pressure coefficient
D	= effective jet diameter
D_n	= nominal jet exit diameter (2.58 cm)
L	= jet-induced lift loss
M	= jet-induced pitching moment
p	= static pressure
q	= dynamic pressure
q_∞	= crossflow dynamic pressure
r	= radius
R	= V_e/V_∞ = jet-to-crossflow velocity ratio
s	= arc length measured along jet trajectory
T	= jet thrust
V_e	= effective jet exit velocity
V_∞	= crossflow velocity
x	= streamwise coordinate
y	= transverse coordinate
z	= coordinate perpendicular to plate

I. Introduction

DURING transition of a jet VTOL aircraft from hover to forward flight, there is a complicated interaction between the jet engine exhaust and the crossflow which results in a change in the pressure loadings on the aircraft in the vicinity of the jet. The integrated effect of these jet-induced pressure loadings is a loss in lift and an incremental moment. Previous wind-tunnel tests have attempted to measure these induced lift losses and moments for specific, proposed VTOL configurations.^{1,2} Many other investigators have studied a geometrically more simple model of such a flowfield—that of a low-speed round jet with uniform initial velocity profile exiting perpendicular to a flat plate into a uniform crossflow. Such efforts have centered around the measurement of jet-induced loads on the flat plate³⁻⁷ and jet trajectories.⁸⁻¹⁰ Fearn and Weston found the jet-to-crossflow velocity ratio, R , to be the key parameter in determining the jet-induced load.³ More recently, Fearn and Weston have modeled such a jet-crossflow interaction as a pair of contrarotating vortices

deflected by the crossflow.¹¹ This model has been used by Dietz in an attempt to predict plate surface pressures based upon the strength and location of the jet vortex pair.¹² A detailed survey of the work on the jet-crossflow interaction, as related to VTOL aerodynamics prior to 1970, has been performed by Margason.¹³

The majority of these model studies have been performed using jets with uniform jet exit dynamic pressure profiles. This is in contrast to the nonuniform jet exhaust velocity profiles found in actual jet engines.¹⁴ Livingston¹⁵ and Ziegler and Wooler¹⁶ have studied the effects of stratified jets with nonuniform jet exit velocity profiles and have found different induced pressure loadings than for a model with uniform initial jet profiles. Also, Gentry and Margason found that for a jet in hover there was a large effect of the jet decay rate upon the induced pressures.¹⁷

In the present work, a systematic study was undertaken into the effects of varying jet decay rate upon the induced pressures, lift loss, and pitching moment for a subsonic circular air jet exiting at right angles to a flat plate into a uniform crossflow. Jet decay rate was varied by altering the positioning of various centerbodies in the jet settling chamber and nozzle. Results show that the presence of a centerbody in the jet nozzle significantly increased jet mixing with the crossflow, increased jet decay rate, and decreased the induced lift loss and moment. Thus, it is recommended that future VTOL model studies should simulate anticipated full-scale jet exit conditions as accurately as possible.

II. Experimental Apparatus and Techniques

Experiments were performed in the 0.92×1.2 m (3×4 ft) test section of an Aerolab closed-circuit low-speed wind tunnel located at Old Dominion University. A 0.92×1.2 m (3×4 ft) flat plate was mounted on struts 10.6 cm from the test section floor. A 2.58-cm (1.016 in.)-diam circular jet exited perpendicular to the flat plate 60 cm back from the round leading edge. A schematic of the flat plate and jet, as located in the test section, is shown in Fig. 1. The air jet was supplied by an air compressor through a 14.2-cm-diam plenum and a smooth 30:1 contraction ratio nozzle. A cross section of the jet nozzle and plenum is shown in Fig. 2. Also shown is the 1.9-cm-diam hemispherical tipped centerbody, or round-ended plug, used to alter the jet exit dynamic pressure profile and decay rate. A similar centerbody with a flat tip was also used. Jet flow rate was measured using a turbine flowmeter and held constant to within 0.2% using an automatic control device.

The angle of attack between the flat plate and the crossflow was less than 0.5 deg with no jet flow for all experiments. The

Received June 3, 1977; presented as Paper 77-596 at the AIAA/NASA Ames V/STOL Conference, Palo Alto, Calif., June 6-8, 1977; revision received Feb. 3, 1978. Copyright © American Institute of Aeronautics and Astronautics, Inc., 1977. All rights reserved.

Index categories: Aerodynamics; Jets, Wakes, and Viscid-Inviscid Flow Interactions.

*Assistant Professor, Mechanical Engineering & Mechanics Dept. Associate Member AIAA.

†Research Assistant, Mechanical Engineering & Mechanics Dept.

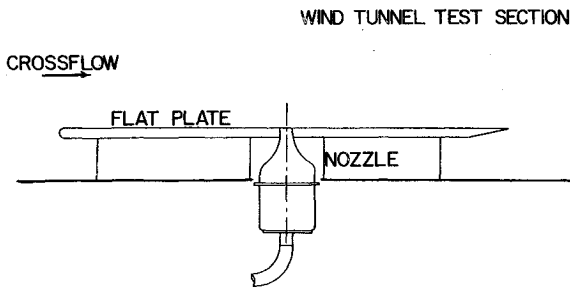


Fig. 1 Schematic of experimental apparatus.

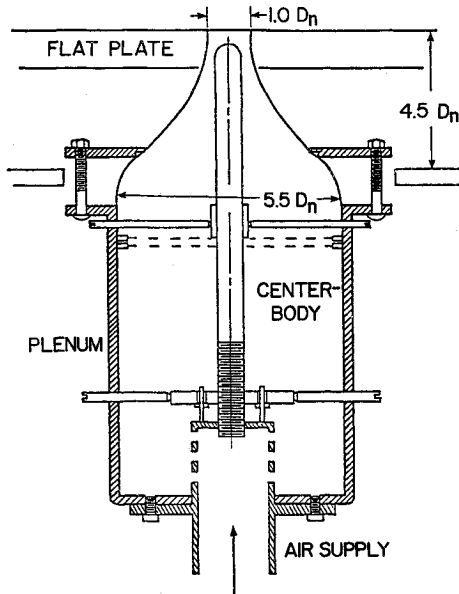


Fig. 2 Cross-sectional view of jet nozzle, plenum, and centerbody.

boundary layer on the plate was artificially tripped using the technique described by Braslow, Hicks, and Harris,¹⁸ and was found to be fully turbulent. A separation bubble was observed at the plate leading edge which extended nominally 8 cm in the transverse and 4-6 cm in the flow directions.

The plate was fitted with 226 pressure ports, 0.061 cm in diameter, located on rays centered at the jet exit. Pressure taps were connected through tubing and scanning valves to a capacitance-type pressure transducer. All pressure transducers were calibrated using a dead-weight tester. Each plate surface pressure measurement was automatically averaged over a minimum of a 5 s interval, since it was found that the pressures at some locations on the plate fluctuated, as observed by Fearn and Weston.³

A three-dimensional probe transverse was fitted to the top of the tunnel test section. A total pressure probe mounted to the traverse was used to locate the jet centerline trajectory. These data were numerically curve-fitted and used to orient a pitot-static probe tangent to the jet for measurement of the jet dynamic pressure along the jet centerline. Temperatures were measured with 0.025-cm-diam chromel-alumel thermocouples. The jet exit temperature was nominally 15°C below the tunnel temperature.

Integrated jet-induced lift losses and pitching moments were numerically calculated using the plate surface pressure data. Constant pressure panels centered at the pressure tap locations were used in the integration. Differences between pressures measured with the jet on and jet off conditions were used.

A technique suggested by Ziegler and Wooler was used to compare data taken with different initial jet velocity profiles.¹⁶ The actual jet exit dynamic pressure was surveyed

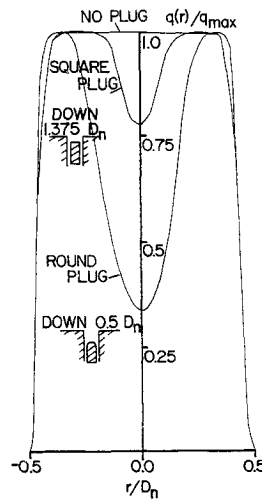


Fig. 3 Examples of non-dimensional jet exit plane dynamic pressure profiles; no crossflow.

for the static case and used to calculate the jet thrust. For comparison purposes, an effective jet velocity and effective jet area were then calculated that represent a slug-flow jet having the measured mass flow rate and thrust, produced by isentropic expansion from the same plenum (stagnation) conditions. This effective initial jet velocity and the tunnel velocity were used to calculate the jet-to-crossflow velocity ratio, R , rather than the conventionally used ratio of dynamic pressures to the one-half power. This resulted in no more than a 6% difference from the value of R calculated in the usual manner, which includes differences in tunnel and jet densities. Since this is within the estimated accuracy of 6% for the experimental R values, the current R values may be considered to be equivalent to those obtained by the conventional definition. The previously mentioned effective jet area was used to calculate an effective circular jet diameter, D . This effective diameter has been used to nondimensionalize the jet centerline trajectory data and jet decay data, as well as the pressure coefficient, lift loss, and pitching moment data.

Jet exit Mach number, based upon the effective jet exit velocity, was equal to 0.4, and jet Reynolds number was 2×10^5 . Tunnel speeds ranged from 13-68 m/s, and the crossflow Reynolds numbers ranged from $7.5 \times 10^5/m$ to $4 \times 10^6/m$.

III. Presentation of Results

Jet-induced plate surface pressures, jet centerline trajectories, and jet dynamic pressure decay data have been measured over a range of jet-to-crossflow ratios of $2.2 < R < 10$. These data have been obtained for the following jet nozzle centerbody configurations: 1) no centerbody; 2) round-ended centerbody with tip submerged one nominal jet exit diameter, D_n , below nozzle exit plane; 3) round-ended centerbody submerged $0.5 D_n$ below nozzle exit; 4) round-ended centerbody flush with nozzle exit; 5) flat-ended centerbody submerged $1.375 D_n$ below nozzle exit; 6) flat-ended centerbody submerged $0.875 D_n$ below nozzle exit; 7) flat-ended centerbody submerged $0.375 D_n$ below nozzle exit; and 8) flat-ended centerbody flush with nozzle exit.

Examples of how the centerbodies affected the jet exit plane dynamic pressure distributions are shown in Fig. 3. These data were taken with no crossflow and the profiles were observed to be axisymmetric. The fore-to-aft symmetry was observed to be destroyed when the crossflow was nonzero. Note that, generally, the closer the centerbody tip was to the nozzle exit plane the more nonuniform the initial dynamic pressure distribution.

Jet-induced plate pressure coefficient data for $R = 3.9$ with no centerbody are compared with data of Fearn and Weston in Fig. 4.³ Lines of constant c_p agree to within the ex-

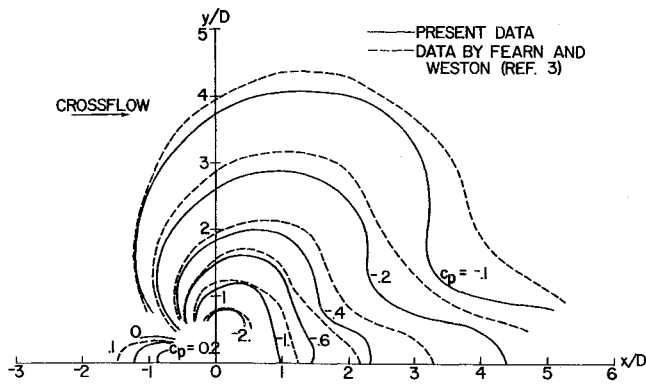


Fig. 4 Constant pressure contour data; no centerbody in nozzle, $R=3.9$.

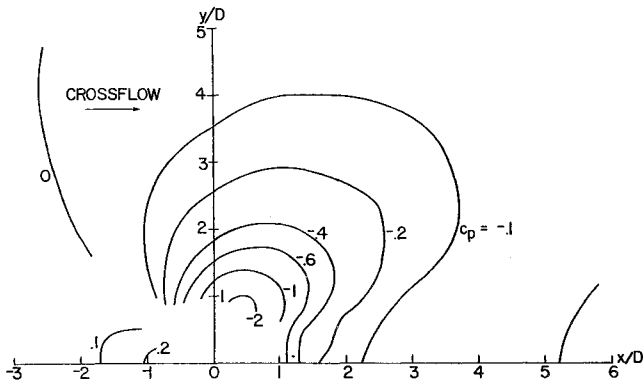


Fig. 5 Constant pressure contour data; flat-ended plug down $0.375 D_n$, $R=4.36$.

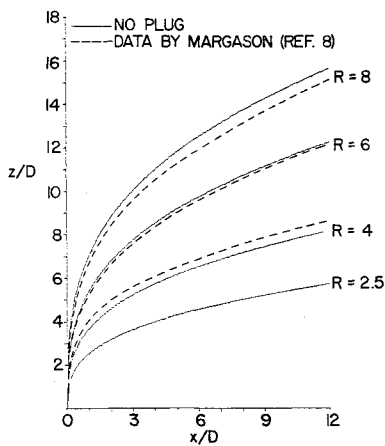


Fig. 6 Jet centerline trajectories for configurations with no centerbody.

perimental accuracy estimated both for the current work and in Ref. 3, except in the region behind the jet.

Pressure coefficient data for a velocity ratio of 4.36 for a configuration with a flat-ended plug submerged 0.375 nominal jet diameters below the jet exit plane are shown in Fig. 5. Through comparison of Figs. 4 and 5, a marked change in the distribution of c_p is observed for a similar value of R when a centerbody is present in the jet nozzle. This change in pressure levels due to the centerbody occurs in the lee of the jet. Similar behavior is observed for other nozzle configurations and velocity ratios.

Nondimensional jet centerline trajectories for varying values of R for jets with no centerbody are shown in Fig. 6. Also shown for comparison are data taken by Margason.⁸ Increasing the crossflow causes the expected increase in jet

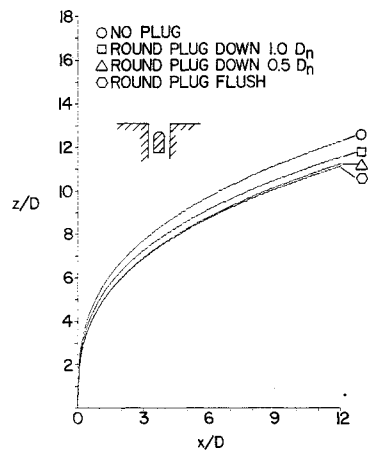


Fig. 7 Jet centerline trajectories for configurations with round-ended centerbodies, $R=6$.

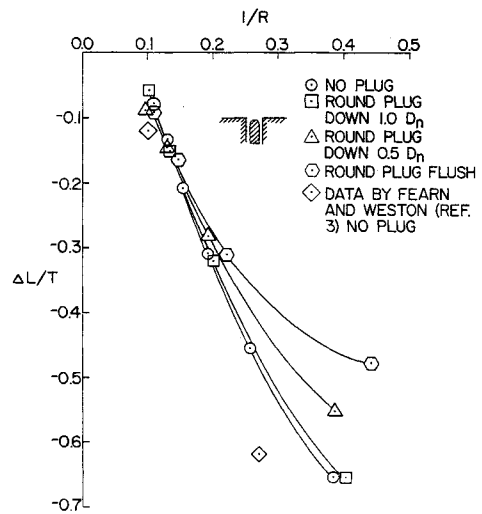


Fig. 8 Integrated lift loss for round-ended plug configurations compared with unplugged jets.

turning. In Fig. 7, nondimensional jet trajectories are shown for a velocity ratio of $R=6.0$ for various centerbody configurations. Note that, generally, the closer the plug tip to the nozzle exit plane, the quicker the jet turning. The same trend is observed at $R=8.0$, but tends to disappear as R decreases below 4.0 .

The integrated lift loss induced by the jet (nondimensionalized by the jet thrust) for various plug configurations is compared with the no-plug case in Figs. 8 and 9. Note that the horizontal axis is the crossflow-to-jet velocity ratio equal to $1/R$. The lift loss has been calculated for a circular area on the plate equal to 43 times the jet effective area. Lift loss increases with increasing crossflow velocity; but for a constant value of R , the presence of a centerbody decreases the lift loss by up to 45% . Also shown in Fig. 8 are approximate integrations of data of Fearn and Weston for comparison with the no-plug configuration.³ Figure 10 compares the jet-induced pitching moment about the nozzle center for the various flat-ended centerbody configurations with the no-plug case. The pitching moment is nondimensionalized by the jet thrust times the jet effective diameter. Here, increased crossflow velocity causes an increase in the pitching moment, and the centerbody decreases the moment.

The nondimensional decay of the jet dynamic pressure for the configuration with no centerbody is presented in Fig. 11 for various values of the jet-to-crossflow velocity ratio, R . As the crossflow increases, the jet decay occurs more rapidly.

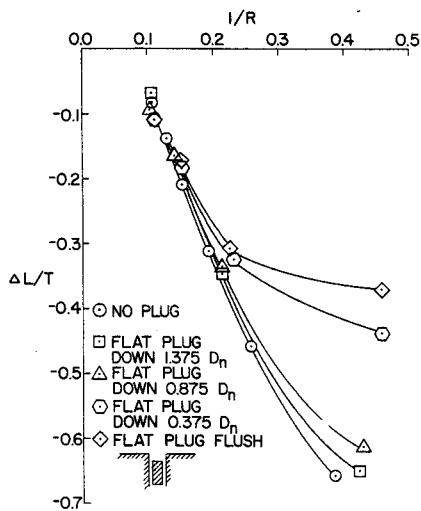


Fig. 9 Integrated lift loss for flat-tipped plug configurations compared with unplugged jets.

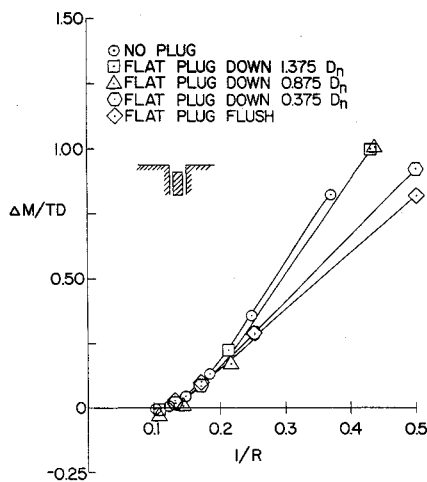


Fig. 10 Pitching moment for flat-ended centerbodies compared with unplugged configurations.

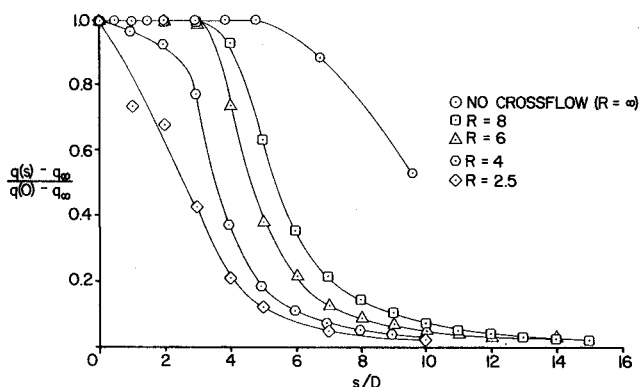


Fig. 11 Dynamic pressure decay along jet trajectory; no centerbody in nozzle.

Figures 12 and 13 show examples of the increased jet decay rate observed as the flat- or round-ended centerbody was moved closer to the nozzle exit plane with the velocity ratio held constant. Similar behavior was observed at all other velocity ratios for which data were obtained. Note that for the examples shown, $R = 4.0$ for the flat-ended centerbody, while $R = 8.0$ for the round-ended centerbody examples. Results are shown on both figures for the case of no centerbody.

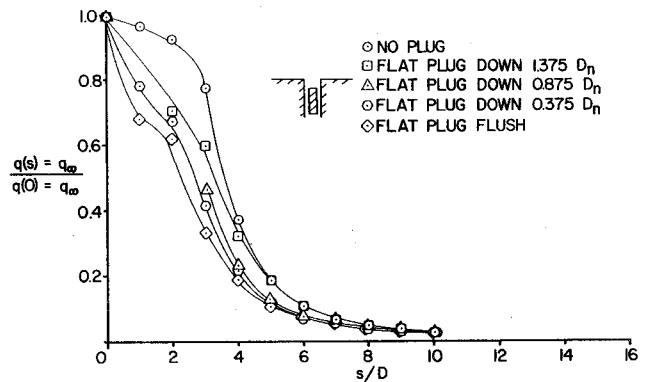


Fig. 12 Dynamic pressure decay along jet trajectory, $R = 4$.

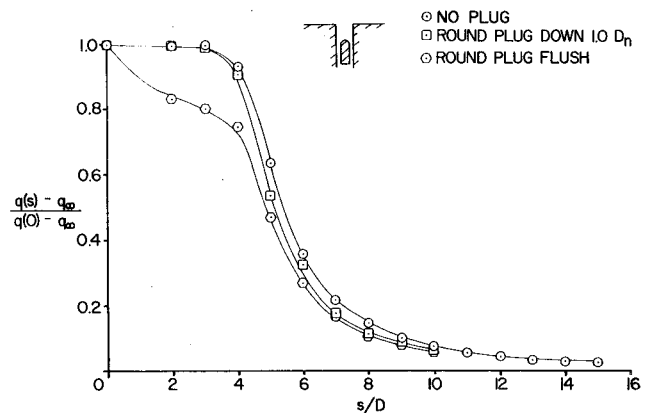


Fig. 13 Dynamic pressure decay along jet trajectory, $R = 8$.

IV. Discussion and Conclusions

All data presented for jet configurations with no centerbody agree well with results presented by previous authors. Development of such a jet is dominated by the jet-to-crossflow ratio, R , as found by Fearn and Weston.³ However, the addition of a centerbody in the jet nozzle will also cause a marked variation in the jet development. Specifically, a centerbody causes nonuniform initial jet dynamic pressure profiles, quicker jet turning, quicker jet decay, and a smaller induced lift loss and pitch moment, assuming the velocity ratio R is held fixed. Based on results of Fearn and Weston,¹¹ it is felt that this observed reduction in induced lift loss, even though the jet turns more quickly and lies closer to the plate, must be due to a weakening of the vortex pair associated with the jet.

Discrepancies between results presented in Ref. 4 and those of other investigators^{3,5-7} are believed to be due to differences in their jet decay rates. The jet used in Ref. 4 was observed to begin to decay more rapidly than jets used in other experiments. Thus, from the current results, it is to be expected that the induced lift loss would be different.

Based upon the current results, where the presence of a centerbody in the nozzle of an air jet entering a crossflow has been found to significantly modify the jet-induced pressure distribution, it is recommended that all future model VTOL studies should duplicate as closely as possible the anticipated jet engine exhaust conditions. It further appears that previous model studies which have had uniform jet exhaust velocity profiles may significantly overestimate the jet-induced lift losses.

Acknowledgment

This work was supported by the NASA Langley Research Center under Grant NSG-47-003-039.

References

- ¹ Vogler, R.D., "Interference Effects of Single and Multiple Round or Slotted Jets on a VTOL Model in Transition," NASA TN D-2380, Aug. 1964.
- ² Margason, R.J. and Gentry, G.L., Jr., "Aerodynamic Characteristics of a Five-Jet VTOL Configuration in the Transition Speed Range," NASA TN D-4812, 1968.
- ³ Fearn, R.L. and Weston, R.P., "The Induced Pressure Distribution of a Jet in a Crossflow," NASA TN D-7916, July 1975.
- ⁴ Ousterhout, D.S., "An Experimental Investigation of a Cold Jet Emitting from a Body of Revolution into a Subsonic Free Stream," NASA CR-2089, Aug. 1972.
- ⁵ Soullier, A., "Testing at Sl. MAS for Basic Investigation in Jet Interactions. Distribution of Pressures Around the Jet Orifice," NASA TTF-14066, April 1968.
- ⁶ Bradbury, L.J.S. and Wood, M.N., "The Static Pressure Distribution Around a Circular Jet Exhausting Normally from a Plane Wall into an Airstream," British Aeronautics Research Council, CP 882, 1965.
- ⁷ Vogler, R.D., "Surface Pressure Distributions Induced on a Flat Plate by a Cold Air Jet Issuing Perpendicularly from the Plate and Normal to a Low Speed Free-Stream Flow," NASA TN D-1629, March 1963.
- ⁸ Margason, R.J., "The Path of a Jet Directed at Large Angles to a Subsonic Free Stream," NASA TN D-4919, Nov. 1968.
- ⁹ Kamotani, Y. and Greber, I., "Experiments on a Turbulent Jet in a Cross Flow," NASA CR-72893, June 1971.
- ¹⁰ Rudinger, G. and Moon, L.F., "Laser-Doppler Measurements in a Subsonic Jet Injected into a Subsonic Cross Flow," *ASME Journal of Fluids Engineering*, Vol. 98, Sept. 1976, pp. 516-520.
- ¹¹ Fearn, R. and Weston, R.P., "Vorticity Associated with a Jet in a Cross Flow," *AIAA Journal*, Vol. 12, Dec. 1974, pp. 1666-1671.
- ¹² Dietz, W.E. Jr., "A Method for Calculating the Induced Pressure Distribution Associated with a Jet in a Crossflow," M.S. Thesis, Florida University, 1975; NASA CR 146434.
- ¹³ Margason, R.J., "Review of Propulsion-Induced Effects on Aerodynamics of Jet/STOL Aircraft," NASA TN D-5617, Feb. 1970.
- ¹⁴ Abbott, W.A., "Studies of Flow Fields Created by Vertical and Inclined Jets When Stationary or Moving over a Horizontal Surface," British Aeronautics Research Council CP-911, 1964.
- ¹⁵ Livingston, D.K., "An Experimental Investigation of a Cold Jet with Solid Center Body Emitting from a Flat Plate into a Subsonic Free Stream," M.S. Thesis, Old Dominion University, May 1975.
- ¹⁶ Ziegler, H and Wooler, P.T., "Analysis of Stratified and Closely Spaced Jets Exhausting into a Crossflow," NASA CR-132297, Nov. 1973.
- ¹⁷ Gentry, G.L. and Margason, R.J., "Jet Induced Lift Losses on VTOL Configurations Hovering In and Out of Ground Effect," NASA TN D-3166, Feb. 1966.
- ¹⁸ Braslow, A.L., Hicks, R.M., and Harris, R.V. Jr., "Use of Grit-Type Boundary-Layer Transition Trips," presented at Conference on Aircraft Aerodynamics, Langley Research Center, May 23-25, 1966, published in NASA SP-124.

From the AIAA Progress in Astronautics and Aeronautics Series...

EXPERIMENTAL DIAGNOSTICS IN GAS PHASE COMBUSTION SYSTEMS—v. 53

*Editor: Ben T. Zinn; Associate Editors: Craig T. Bowman,
Daniel L. Hartley, Edward W. Price, and James F. Skifstad*

Our scientific understanding of combustion systems has progressed in the past only as rapidly as penetrating experimental techniques were discovered to clarify the details of the elemental processes of such systems. Prior to 1950, existing understanding about the nature of flame and combustion systems centered in the field of chemical kinetics and thermodynamics. This situation is not surprising since the relatively advanced states of these areas could be directly related to earlier developments by chemists in experimental chemical kinetics. However, modern problems in combustion are not simple ones, and they involve much more than chemistry. The important problems of today often involve nonsteady phenomena, diffusional processes among initially unmixed reactants, and heterogeneous solid-liquid-gas reactions. To clarify the innermost details of such complex systems required the development of new experimental tools. Advances in the development of novel methods have been made steadily during the twenty-five years since 1950, based in large measure on fortuitous advances in the physical sciences occurring at the same time. The diagnostic methods described in this volume—and the methods to be presented in a second volume on combustion experimentation now in preparation—were largely undeveloped a decade ago. These powerful methods make possible a far deeper understanding of the complex processes of combustion than we had thought possible only a short time ago. This book has been planned as a means of disseminating to a wide audience of research and development engineers the techniques that had heretofore been known mainly to specialists.

671 pp., 6x9, illus., \$20.00 Member \$37.00 List

TO ORDER WRITE: Publications Dept., AIAA, 1290 Avenue of the Americas, New York, N.Y. 10019